Original Research Article

Selenium reduces hepatopancreas lipid accumulation of grass carp (*Ctenopharyngodon idella*) fed high-fat diet via lipophagy activation

Xiaotian Zhang, Haibo Yu[*], Xianfang Yan, Pengju Li, Chi Wang, Cheng Zhang, Hong Ji

College of Animal Science and Technology, Northwest A&F University, Yangling 712100, China

A B S T R A C T

It has been reported that selenium (Se) can reduce hepatopancreas lipid accumulation induced by high-fat diet. However, its mechanism is still unknown. This study aims to investigate the specific mechanisms by which Se alleviates high-fat diet-induced lipid accumulation. Grass carp were fed control diet (4.8% lipid, Con), high-fat diet (8.8% lipid, HFD) or HFD supplemented with 0.3 mg/kg nano-Se (HSe0.3) for 10 weeks. Growth performance, Se deposition, lipid accumulation, hepatic ultrastructure, and gene and protein expression levels associated with autophagy were examined. Furthermore, oleic acid (OA) was used to incubate the grass carp hepatocytes (L8824) for 24 h, and then the L8824 were incubated with sodium selenite in presence or absence of an autophagy inhibitor for 24 h. L8824 was analyzed for triglyceride concentration, immunofluorescence, and gene and protein expression levels associated with autophagy. We found that dietary nano-Se improved the growth of fish fed HFD and also decreased hepatosomatic index and intraperitoneal fat ratio of fish fed HFD ($P < 0.05$). HFD significantly increased hepatopancreas lipid accumulation and decreased autophagic activity ($P < 0.05$). Treatment of grass carp fed HFD with nano-Se decreased lipid accumulation and restored hepatic autophagy ($P < 0.05$). In vitro, Se (100 μM sodium selenite) obviously activated autophagy in L8824 incubated with OA, and consequently reduced the lipid accumulation induced by OA ($P < 0.05$). Furthermore, using pharmacological inhibition (chloroquine) of the autophagy greatly diminished the beneficial effects of Se on alleviating OA-induced lipid accumulation and increased the co-localization of lipid droplets with autophagosome ($P < 0.05$), which indicated that Se increased autophagic flux. In conclusion, these results suggest that Se alleviates HFD-induced hepatopancreas lipid accumulation by activating lipophagy.

1. Introduction

Lipids not only provide energy for fish, but also act as components of cell membranes and provide essential fatty acids for fish (Jia et al., 2020a; Li et al., 2016). Appropriately increasing the lipids content of diet can exert a protein-sparing effect, which not only promotes fish growth and reduces nitrogen emissions, but also reduces feed costs. Therefore, the use of high-fat diet (HFD) in aquaculture is becoming increasingly common (Chen et al., 2016; Li et al., 2012; Ma et al., 2018; Xie et al., 2020). However, excessive lipid addition to diet has negative effects on the growth and health of farmed fish. Long-term intake of HFD causes excessive lipid accumulation in fish, producing reactive oxygen species, inflammation, and oxidative stress, which eventually leads to impaired growth performance or even death (Cao et al., 2020; Chen et al., 2016; Lu et al., 2013a; Xie et al., 2020; Zhao et al., 2019). At present, there are problems such as excessive lipid accumulation, abnormal blood lipids, liver damage, and decreased resistance to adversity in farmed fish, which have caused extremely serious losses to the aquaculture (Deng et al., 2018; Lu et al., 2013a). Therefore, it is particularly important to explore methods to reduce the negative effects of HFD on fish.

Selenium (Se) is an essential micronutrient for animals. It plays an important role in maintaining normal physiological functions, preventing protein and lipid damage, and exerting anti-inflammatory and antioxidant functions. Especially, because of its

* Corresponding author.
E-mail address: yuhaiboper@nwsuaf.edu.cn (H. Yu).

Peer review under responsibility of Chinese Association of Animal Science and Veterinary Medicine.

Production and Hosting by Elsevier on behalf of KeAi

effective antioxidant properties, it has attracted much attention (Avery and Hoffmann, 2018; Khurana et al., 2019; Kursvietiene et al., 2020; Wang et al., 2017b). The bioavailability of Se is related to its form. Compared with other conventional types of Se, nano-Se shows better potential because of its high bioavailability and low toxicity (Ibrahim et al., 2021; Sarkar et al., 2015). It has been reported that Se ameliorates HFD-induced dyslipidemia in mice (Gao et al., 2020; Yi et al., 2020). And similarly in fish, Se also reduces serum triglyceride (TG) and cholesterol (TC) levels in Nile tilapia (*Oreochromis niloticus*) and blunt snout bream (*Megalobrama amblycephala*) (Durigon et al., 2019; Ghazi et al., 2022; Hao et al., 2020; Ibrahim et al., 2021). It was consistent with our past research (Liu et al., 2021) in which nano-Se could relieve excessive lipid accumulation in grass carp fed HFD. However, the detailed mechanism of how Se exerts its lipid-lowering effect is still unknown.

Autophagy is a degradation pathway that breaks down and re-cycles intracellular components through lysosomes. It removes misfolded proteins and damaged organelles and participates in energy metabolism, which is essential for cells to maintain normal functions and adapt to environmental stress (Flores-Toro et al., 2016; Xia et al., 2019; Zhang et al., 2018; Zhao et al., 2020). Lip-ophagy is a type of selective autophagy, which specifically trans-ports lipid droplets (LD) to lysosomes for degradation. Previous studies showed that lipophagy played an important role in lipid metabolism and energy homeostasis in the mammals (Cisa-Wieczorek and Hernandez-Alvarez, 2020; Singh et al., 2009). Whereas the lack of lipophagy leads to hepatic steatosis, but the activation of lipophagy can reduce the subsequent liver injury and steatosis (Lu and Cederbaum, 2015). Wang et al. (2018) first verified the presence of lipophagy in zebrafish liver. They found that inhibiting the lipophagy of zebrafish hepatocyte line significantly increased the number of LD and decreased fatty acid β-oxidation in zebrafish hepatocyte line cells, demonstrating that lipophagy plays an important regulatory role in lipolysis to fish (Wang et al., 2018, 2019). In mammalian and fish studies, persistent lipid overload due to long-term feeding of HFD inhibits autophagy, which in turn re-duces the role performed by lipophagy in lipid metabolism and exacerbates lipid accumulation in the organism (Ueno and Komatsu, 2017; Wu et al., 2019; Zhang et al., 2018). It has been reported that zinc alleviated copper-induced lipotoxicity by pro-moting the occurrence of hepatic lipophagy (Wei et al., 2021). Therefore, activating lipophagy may be an effective strategy to alleviate lipid accumulation. Previous study has shown that sodium selenite significantly improves cardiac autophagic activity and thus attenuates HFD-induced cardiac injury for mice (Zhang et al., 2019). In addition, selenite can also promote mitophagy in mammalian cells (Li et al., 2015). However, whether Se can reduce hepatic lipid accumulation in grass carp by activating lipophagy has not been reported yet.

Grass carp (*Ctenopharyngodon idella*) is one of the most pro-ductive farmed fish around the world. In 2020, the production of grass carp in China alone exceeds 5.5 million tonnes (Lu et al., 2022; Wu et al., 2012). However, with the widespread use of HFD, excessive lipid accumulation has become one of the biggest chal-lenges in grass carp culture (Tian et al., 2021). Therefore, in this study, we investigate the specific mechanism of Se in reducing HFD-induced hepatopancreas lipid accumulation in grass carp.

2. Materials and methods

2.1. Animal ethics

The experiment procedures were conducted in compliance with the Guidelines for Animal Research which was approved by the Animal Care Committee of Northwest A&F University, Yangling, China (No. DKXT20200930).

2.2. Experimental diets

In this experiment, three experimental diets were configured, including control diet (4.8% lipid, Con), high-fat diet (8.8% lipid, HFD) and HFD supplemented with 0.3 mg/kg nano-Se (HSe0.3). Based on the previous studies, the amount of nano-Se added to the diets was 0.3 mg/kg (Liu et al., 2021). And, the lipid content of control diet and high-fat diet was based on previous studies (Guo et al., 2015, 2022; Xiao et al., 2017). The nano-Se (>99% purity) (average particle size 60 nm) was purchased from Guangzhou Bosar Biochemical Tech-nology Research Co., Ltd (Guangzhou, China). Selenium contents in the different diets were measured using liquid chromatography coupled with atomic fluorescence spectroscopy (LC-AFS) (Beijing Haiguang Instrument Co., Ltd, China), and there were 0.08, 0.08, and 0.38 mg Se/kg for the control, HFD, and HSe0.3 diets, respectively. Diet ingredients, including Se, were crushed and well mixed, and pellets with a diameter of 2.0 mm were extruded using a pelleting machine, then the pellets were crushed to make crushed diet with a smaller diameter (0.6 to 2.0 mm). And then, the diets were air dried to approximately 10% moisture in a ventilated cool place and stored at −20 °C until use. The ingredients and proximate composition of diets are shown in Table 1.

2.3. Fish and experimental conditions

Grass carp were obtained from the Changsheng Fish Hatchery (Beijing, China). Before the experiment, the grass carp were

Table 1
The composition of experimental diets (g/kg, air-dry basis).

Item	Groups		
	Con	HFD	HSe0.3
Ingredients			
Fish meal	50	50	50
Soybean meal	250	250	250
Rape cake	160	160	160
Cottonseed meal	160	160	160
Wheat flour	170	170	170
DDGS	50	50	50
Rice bran	60	60	60
Soybean oil	10	50	50
Choline chloride	5	5	5
$Ca(H_2PO_4)_2$	20	20	20
Microcrystalline cellulose	44.9	4.9	4.9
Vitamin mixture[1]	10	10	10
Mineral mixture[2]	10	10	10
Antioxidant	0.1	0.1	0.1
Proximate composition analysis			
Moisture	99	97	110
Crude protein	316	315	314
Crude lipid	42	83	81
Crude ash	71	66	70
Crude protein to energy ratio, g/MJ	16.8	15.7	15.7
Gross energy, MJ/kg	18.8	20.1	20.1
Se, mg/kg	0.08	0.08	0.38

Con = control diet; HFD = high fat diet; HSe0.3 = HFD supplemented with 0.3 mg/kg nano-Se; DDGS = distillers dried grains with soluble.

[1] Vitamin premix (per kilogram of diet): vitamin A, 3000 IU; vitamin E, 60 IU; vitamin D, 2000 IU; vitamin C, 200 mg; thiamine, 5 mg; riboflavin, 10 mg; mena-dione, 10 mg; pyridoxine·HCl, 10 mg; cyanocobalamin, 0.02 mg; biotin, 1 mg; calcium pantothenate, 40 mg; folic acid, 5 mg; niacin, 100 mg; inositol, 200 mg. Cellulose was used as a carrier.

[2] Mineral mix (per kilogram of the total mineral): $KAl(SO_4)_2$, 1.59 g; $CaCO_3$, 181.01 g; $Ca(H_2PO_4)_2$, 446.01 g; $CoCl_2$, 0.70 g; $MgSO_4$, 52.16 g; $MnSO_4·H_2O$, 0.70 g; KCl, 165.53 g; KI, 0.14 g; $ZnCO_3$, 1.92 g; NaH_2PO_4, 136.05 g; Na_2SeO_3, 0.06 g; $CuSO_4·5H_2O$, 0.75 g; Ferric citrate, 13.38 g.

domesticated in a recirculating aquarium at a water temperature of 26 °C and fed the control diet three times a day. After 2 weeks of acclimatization, 135 healthy grass carp with similar size (mean weight = 3.45 ± 0.02 g) were randomly assigned to 9 tanks (70 L) of a recirculating culture system. Grass carp were separated into 3 groups with 3 replicates per treatment and 15 fish per replicate. Fish were fed each diet three times a day for 10 weeks. The water temperature was maintained at 26 °C during the feeding experiment. Ammonia nitrogen and nitrite nitrogen were kept below 0.10 and 0.05 mg/L, respectively.

2.4. Sample collection and calculations

At the end of the feeding experiment, all the fish were fasted for one day and anaesthetized with MS-222 (90 mg/L) before sampling (Li et al., 2016). Fish in each tank were counted and weighed to calculate weight gain rate (WGR), specific growth rate (SGR), and feed conversion ratio (FCR). Body length of grass carp was measured to calculate condition factor (CF). Blood drawn from the tail vein was stored at 4 °C for 6 h and supernatant was stored at −80 °C after centrifugation (4 °C, 860 × g for 10 min). After blood collection, 9 fish were randomly selected, and dorsal white muscle, hepatopancreas and abdominal fat were taken and stored at −80 °C after rapid freezing in liquid nitrogen for determination of Se content as well as extraction of tissue RNA, protein and tissue homogenate for subsequent determination. Three fish were randomly selected, and hepatopancreas was taken and stored in 4% paraformaldehyde (Beyotime, China) for making tissue sections. For the remaining fish, hepatopancreas was taken and preserved in electron microscope fixative (2% paraformaldehyde + 2.5% glutaraldehyde) (Leagene, China), which was used to make electron microscope sections. During this period, the weight of empty shell, hepatopancreas, and abdominal fat were measured for calculating viscero-somatic index (VSI), hepato-somatic index (HSI), and intraperitoneal fat ratio (IPF). The following equations were used.

$$\text{Weight gain rate (WGR, \%)} = (w_t − w_0)/w_0 × 100$$

$$\text{Specific growth rate (SGR, \%/day)} = (\ln w_t − \ln w_0)/\text{day} × 100$$

$$\text{Feed conversion ratio (FCR, g/g)} = \text{FI}/(w_t − w_0)$$

$$\text{Condition factor (CF, g/cm}^3) = w_t/\text{BL}^3 × 100$$

$$\text{Viscero − somatic index (VSI, \%)} = w_v/w_t × 100$$

$$\text{Hepato − somatic index (HSI, \%)} = w_h/w_t × 100$$

$$\text{Intraperitoneal fat ratio (IPF, \%)} = w_a/w_t × 100$$

In the equations, w_t, w_0 are the final and initial grass carp weights (g); FI is the average tail feed intake (g); BL is the final grass carp body length (cm); w_v, w_h, w_a are the weights of viscera (g), hepatopancreas (g), and abdominal fat (g), respectively.

2.5. Testing of serum and hepatopancreas parameters

Hepatopancreas samples were homogenized in pre-cooled phosphate-buffered saline solution (PBS) (Cytiva, USA) diluted at 1:9 (wt:vol). The supernatant was stored at −80 °C after centrifugation (4 °C, 860 × g for 10 min). The content of serum TG, TC and hepatopancreas TG were measured using a commercial kit (Nanjing Jiancheng Bioengineering Institute, China). Protein concentrations of hepatopancreas supernatant were measured using a BCA protein assay kit (Solarbio, China).

2.6. Analysis of Se content in tissues

Acid digestion was carried out in a microwave digestion system. The samples were digested using acid mixture (the ratio of HNO_3 to H_2O_2 = 5:1). The completely digested samples were cooled to room temperature, and then 5 mL of a 6 M HCl (50%) solution was added and heated to 110 °C until 1 mL of liquid remained. The final volume was fixed to 50 mL for further Se analysis by LC-AFS (Beijing Haiguang Instrument Co., Ltd, China) (Kumar et al., 2017; Kumar and Singh, 2019). A Se calibration standard solution was used to prepare a standard curve ($R^2 > 0.999$).

2.7. Histological analysis

Samples for light microscopic observation were fixed in 4% paraformaldehyde (Beyotime, China) for 24 h, dehydrated in a gradient concentration of ethanol solution, paraffin embedded and cut into 5 μm thick sections using a rotary block cutter. The sections were then stained with hematoxylin and eosin (H&E) and observed under a microscope (Nikon, Japan).

Samples for electron microscopic observation were fixed in electron microscope fixative (2% paraformaldehyde and 2.5% glutaraldehyde) (Leagene, China) for 24 h, rinsed in PBS and then fixed in 1% osmium acid for 2 h. Samples were dehydrated in a gradient concentration of ethanol solution, successively transparent and embedded using white glue, and polymerized in an oven for 48 h (Lu et al., 2013b). Samples were trimmed with a block trimmer (Leica, Germany), cut into ultrathin sections using an ultrathin sectioning machine (Leica, Germany), stained with uranyl acetate and lead citrate. Finally, samples were observed under a transmission electron microscope (FEI, USA).

2.8. Cell culture and treatments

Grass carp hepatocytes (L8824) (China Center for Type Culture Collection, China) were cultured in minimum essential medium (Cytiva, USA) containing 10% fetal bovine serum (Tianhang, China) at 27 °C and 5% CO_2. Medium was changed every 24 h and passages were performed every 72 h.

Hepatocytes were exposed to 300 μM oleic acid (OA) for 24 h to create an in vitro model. To identify the function of lipophagy in the reduction of lipid accumulation in grass carp hepatocytes by Se, L8824 cells were treated with the Se or an autophagy inhibitor chloroquine (CQ) (Selleck, USA) for 24 h. Treatments were carried out as follows: Control (no additional addition), OA (300 μM OA), OA + CQ (300 μM OA + 50 μM CQ), OA + Se (300 μM OA + 100 μM Na_2SeO_3), and OA + Se + CQ (300 μM OA + 100 μM Na_2SeO_3 + 50 μM CQ).

2.9. Determination of cell TG content and Nile Red staining

The content of TG in L8824 cell was measured using a commercial kit (Applygen, China). Protein concentration of L8824 was measured using the BCA Protein Concentration Assay Kit (Solarbio, China).

The cell was washed with PBS (Cytiva, USA) and fixed with 4% paraformaldehyde (Beyotime, China) for 30 min. Then a lipid fluorescent staining kit (Nile Red Method) (Solarbio, China) was used to stain cellular lipids. Finally, sample was observed under an inverted fluorescence microscope.

2.10. Immunofluorescence co-localization

The co-localization of LD and autophagosomes in hepatocytes was detected using immunofluorescence. L8824 cells were fixed with 4% paraformaldehyde (Beyotime, China) for 15 min, then samples were permeabilized and blocked with Immunostaining Permeabilization Solution with Triton X-100 and QuickBlock Blocking Buffer for Immunol Staining (Beyotime, China). Next, samples were incubated with autophagy marker protein microtubule-associated protein light chain-3 (LC3) antibody (1:400, Wanleibio, China) overnight at 4 °C. On the next day, the samples were incubated with Alexa Fluor 647-labeled goat anti-rabbit IgG (1:500, Beyotime, China) secondary antibody. The LD were stained with BODIPY 493/503 (Glpbio, USA) and nuclei were stained with 4,6-diamidino-2-phenylindole (DAPI) (Bioworld, USA). Images were taken by laser scanning confocal microscopy (Leica, Germany).

2.11. RNA isolation and quantitative real-time PCR

The method was described in our previous study (Liu et al., 2022). Total RNA was extracted from hepatopancreas using Trizol reagent (Accurate, China), and then samples were assayed for quality and concentration using a multifunctional enzyme marker (BioTek, USA). Finally, RNA was reverse transcribed to cDNA using a reverse transcription kit (Vazyme, China).

Expression levels of selected genes were assessed by quantitative real-time PCR. Quantitative real-time PCR assays were performed using ChamQ SYBR qPCR Master Mix (Vazyme, China) and quantified on a thermal cycler (Roche, Switzerland). The 20 μL reaction mixture contained: 2× ChamQ SYBR qPCR Master Mix 10.0 μL, forward primer (10 μM) 0.4 μL, reverse primer (10 μM) 0.4 μL, ddH$_2$O 7.2 μL, template cDNA 2 μL, and then use the followed program: pre-denaturation at 95 °C for 3 min, followed by 40 amplification cycles of 10 s at 95 °C, 30 s at 60 °C, and finally with a melting curve analysis. For each sample, gene expression was corrected by β-actin and the relative expressions of genes were calculated by the $2^{-\Delta\Delta Ct}$ method (Deng et al., 2018). All amplification efficiency of primers was between 96% and 103%. The primers are shown in Table 2.

2.12. The Western blotting

The Western blotting method was referenced to our recent study (Zhang et al., 2022). Briefly, hepatopancreas lysates were prepared using RIPA buffer (Solarbio, China), and then the sample

protein concentrations were standardized. Protein samples were separated by sodium dodecyl sulfate-polyacrylamide gel electrophoresis (SDS-PAGE) and transferred to polyvinylidene fluoride membranes (PVDF) (Millipore, USA) for protein blotting analysis. After incubation of the membrane with primary and secondary antibodies, blots were observed using ECL Super Sensitive Kit (Di Ning, China), and protein bands were quantified using Gel-pro analyzer software. The following antibodies were used: antibodies against LC3 (1:800, Wanleibio, China), antibodies against sequestosome 1 (P62) (1:1000, Wanleibio, China), antibodies against autophagy related 5 (ATG5) (1:1000, Abmart, China), antibodies against beta-actin (1:1000, Bioss, China), and antibodies against glyceraldehyde-3-phosphate dehydrogenase (GAPDH) (1:2000, Servicebio, China).

2.13. Statistical analysis

All results were presented as mean ± SD (standard deviation). A two-tailed *t*-test or a one-way ANOVA and then Duncan's multiple range test were done to analyze the data by SPSS 26.0 (SPSS Inc., USA). Before all analyses, all data were tested by homogeneity of variance test (Levene's test). Differences between data were considered significant when the *P*-value was less than 0.05. GraphPad Prism 8.0 (GraphPad Inc., USA) was used for plotting.

3. Results

3.1. In vivo studies

3.1.1. The effect of dietary Se on growth performance and biological performance of grass carp fed HFD

After the 10-week of feeding, the survival rates of grass carp in all treatment groups were 100%. In this study, compared to the Con group, the final body weight (FBW), WGR and SGR of grass carp fed HFD was significantly decreased (*P* < 0.05) (Fig. 1A to C), while FCR, VSI, HSI, IPF and CF in HFD group were significantly increased (*P* < 0.05) (Fig. 1D to H). However, dietary Se significantly reduced the increase of the FCR, VSI, HSI, IPF and CF caused by HFD (*P* < 0.05) (Fig. 1D to H) and significantly increased the FBW, WGR and SGR (*P* < 0.05) (Fig. 1A to C).

3.1.2. The effect of dietary Se on Se deposition in hepatopancreas and muscle of grass carp fed HFD

Compared with the Con and the HFD groups, the Se content in hepatopancreas and muscle of grass carp in HSe0.3 group was significantly increased (*P* < 0.05) (Fig. 2). Selenium deposition in

Table 2
List of PCR primer sequences for real-time PCR analysis.

Gene	Primer sequences (5′ to 3′)	Accession no.	Amplicon size, bp	E-values, %	R^2
β-Actin	F: CGTGACATCAAGGAGAAG	M25013	299	99.7	0.994
	R: GAGTTGAAGGTGGTCTCAT				
Beclin1	F: GCTGTCCCAACTACCAGAAG	MN311523	105	97.6	0.996
	R: CCCTCAATGCTCTCCAGTTC				
LC3	F: CTCCAGCTCAACTCCAACCA	MG821471	193	100.1	0.998
	R: CTGAGGACACGCAGTTCCAA				
ATG5	F: CACGGAGAGAGAAGCAGAGC	MK635464	119	96.5	0.988
	R: AGCGTGGAGGTCAAACAACA				
ATG7	F: CGGCACAGCATCATCTTTCG	MG797681	170	96.5	0.995
	R: GCCAGCCTTTTAGGGTCCAT				
ATG12	F: GCTGTTGAAGGCTGTCGGT	MK635465	165	98.0	0.985
	R: TGGTGATGGAGCAAATGACTGA				
Rab7	F: GCACTCAAACAGGAAACCGA	MF598474	90	97.0	0.993
	R: TGCTGATGGCTTGGCTCTAT				

Beclin1 = autophagy-related gene 6; *LC3* = microtubule-associated protein light chain 3; *ATG5* = autophagy related gene 5; *ATG7* = autophagy related gene 7; *ATG12* = autophagy related gene 12; *Rab7* = ras-related protein 7; F = forward primer; R = reverse primer.
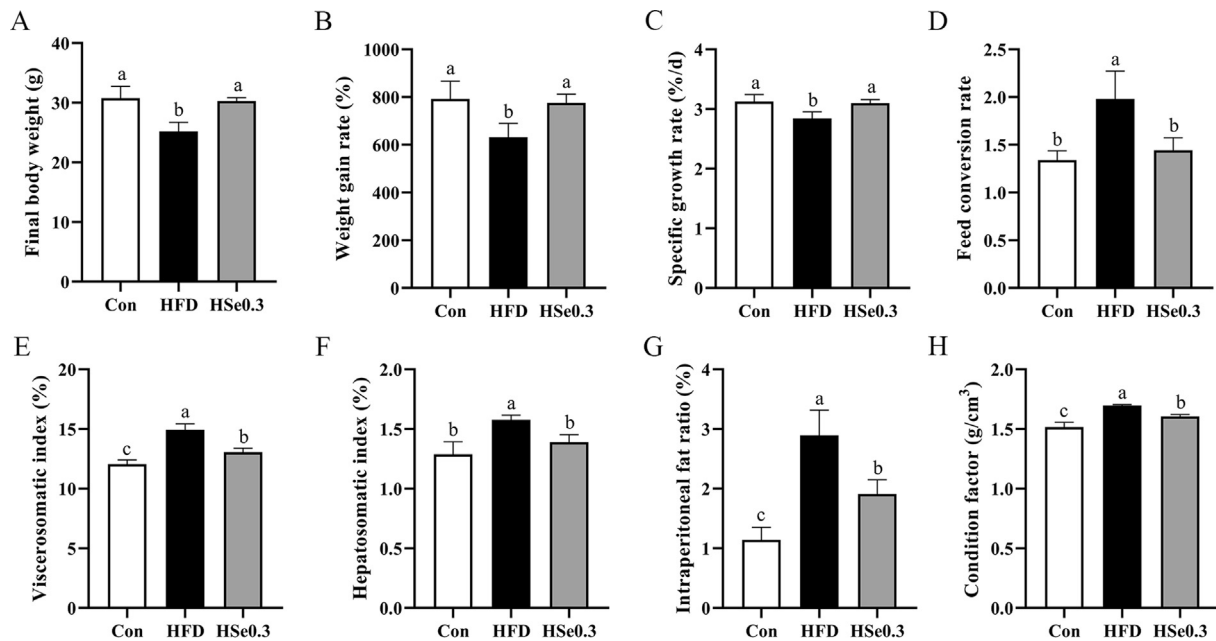
Fig. 1. Effect of dietary Se on growth and biomorphology of grass carp fed with HFD. (A) Final body weight (FBW). (B) Weight gain rate (WGR). (C) Specific growth rate (SGR). (D) Feed conversion rate (FCR). (E) Viscerosomatic index (VSI). (F) Hepatosomatic index (HSI). (G) Intraperitoneal fat ratio (IPF). (H) Condition factor (CF). All results are shown as mean $\pm$ SD, $n = 3$. Different letters indicate significant differences based on one-way ANOVA by Duncan's test ($P < 0.05$). Con = control diet; HFD = high-fat diet; HSe0.3 = HFD supplemented with 0.3 mg/kg nano-Se.
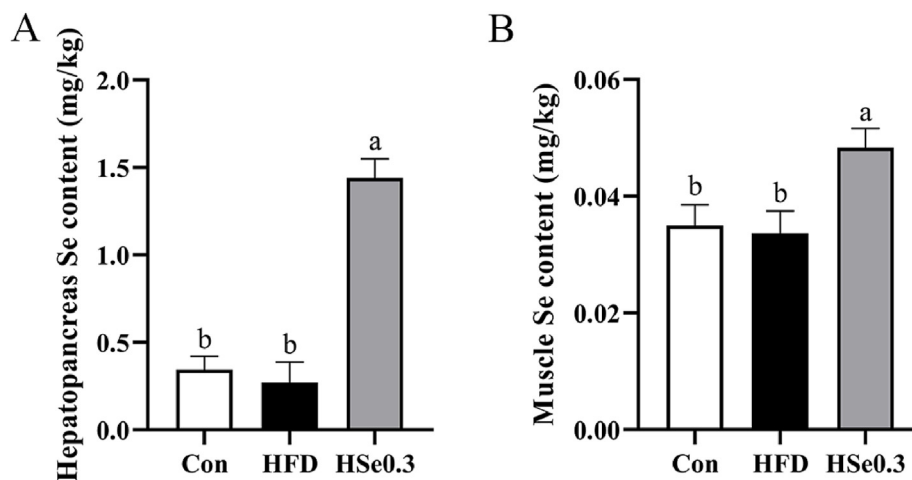
Fig. 2. Effect of dietary Se on Se deposition in grass carp fed with HFD. (A) Se deposition in hepatopancreas of grass carp. (B) Se deposition in muscle tissue of grass carp. All results are shown as mean $\pm$ SD, $n = 6$. Different letters indicate significant differences based on one-way ANOVA by Duncan's test ($P < 0.05$). Con = control diet; HFD = high-fat diet; HSe0.3 = HFD supplemented with 0.3 mg/kg nano-Se.

grass carp hepatopancreas of HSe0.3 group was about three times higher than the other treatment groups (Fig. 2A). Compared to the Con group, the Se content in grass carp hepatopancreas and muscle tissue of HFD group tended to decrease, but no significant difference was observed ($P > 0.05$) (Fig. 2).

3.1.3. The effect of dietary Se on lipid deposition of grass carp fed HFD

The results showed that serum TG, TC, and hepatopancreas TG content in grass carp fed HFD were higher compared with Con group, while dietary Se significantly improved the phenotype of hepatopancreas lipid accumulation ($P < 0.05$) (Fig. 3A to C). These

results were confirmed by hepatopancreas H&E staining sections, and less LD were observed in HSe0.3 group (Fig. 3D). In conclusion, HFD induced lipid accumulation in grass carp hepatopancreas, whereas Se relieved hepatopancreas lipid accumulation.

3.1.4. The effect of dietary Se on hepatopancreas autophagy of grass carp fed HFD

The autophagic pathways in hepatopancreas were measured by the image of hepatopancreas ultrastructure, the quantification of related gene expression, and Western blotting (Fig. 4). The hepatopancreas ultrastructure results showed that the areas of LD in HFD group were larger than those in Con and HSe0.3 groups, and
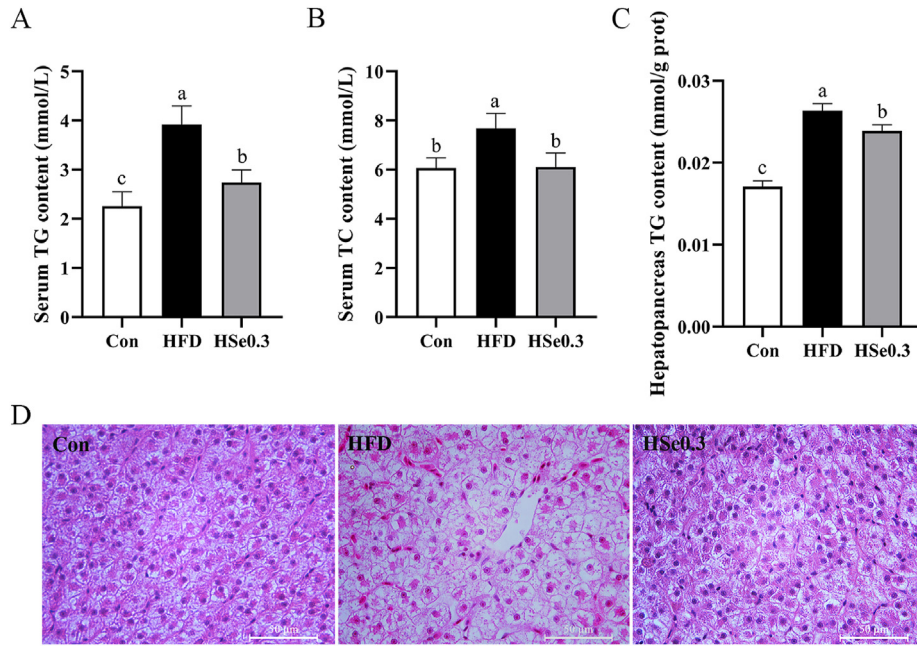
Fig. 3. Effect of dietary Se on hepatopancreas lipid deposition in grass carp fed with HFD. (A) Content variation of serum triglyceride (TG) content in grass carp. (B) Content variation of serum cholesterol (TC) content in grass carp. (C) Content variation of TG in hepatopancreas tissue of grass carp. (D) Histopathological examination by H&E staining for hepatopancreas of grass carp. All results are shown as mean ± SD, $n = 6$. Different letters indicate significant differences based on one-way ANOVA by Duncan's test ($P < 0.05$). Con = control diet; HFD = high-fat diet; HSe0.3 = HFD supplemented with 0.3 mg/kg nano-Se.
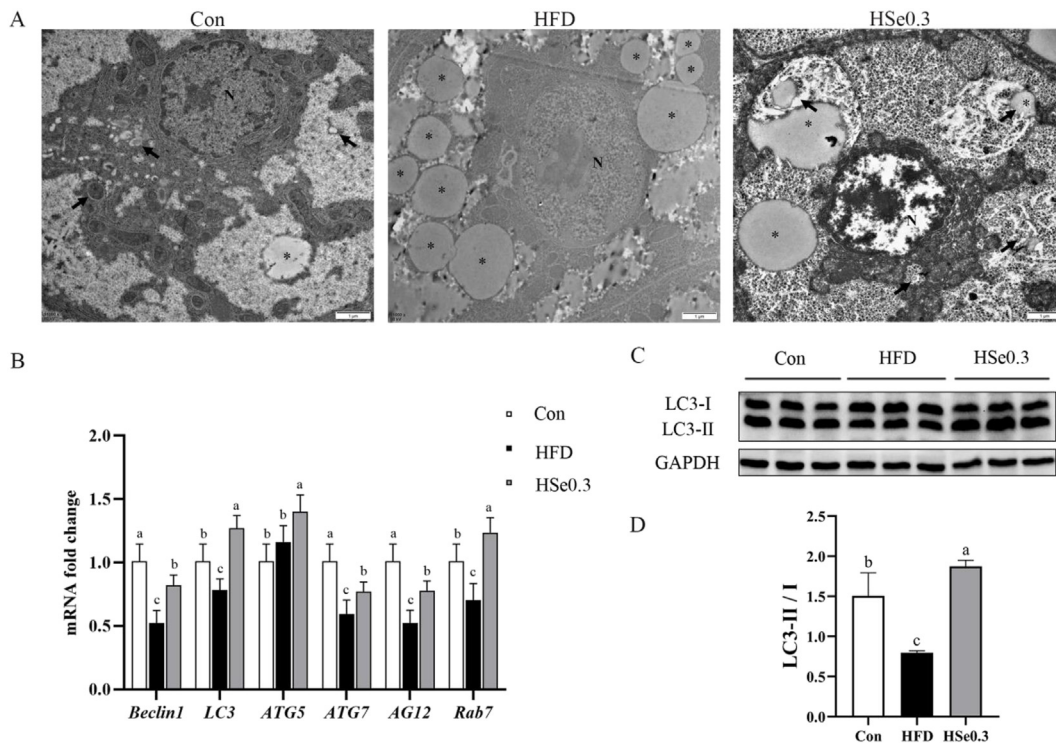

Fig. 4. Effect of dietary Se on the hepatopancreas autophagy of grass carp fed with HFD. (A) Transmission electron microscope (TEM) images of the structural organization of grass carp hepatocytes. The black asterisk in figures represents the lipid droplets; the black arrow in figures represents the autophagy; N, nucleus. (B) Expression of autophagy-related genes in hepatopancreas of grass carp. (C) Image of autophagy marker proteins in the hepatopancreas evaluated by Western blotting analysis. (D) Relative quantification of protein LC3-II to LC3-I. All results are shown as mean ± SD, $n = 6$. Different letters indicate significant differences based on one-way ANOVA by Duncan's test ($P < 0.05$). Con = control diet; HFD = high-fat diet; HSe0.3 = HFD supplemented with 0.3 mg/kg nano-Se; Beclin1 = autophagy-related gene 6; LC3 = microtubule-associated protein light chain 3; ATG5 = autophagy-related gene 5; ATG7 = autophagy-related gene 7; ATG12 = autophagy-related gene 12; Rab7 = ras-related protein 7; LC3 = microtubule-associated protein light chain 3; GAPDH = glyceraldehyde-3-phosphate dehydrogenase.

there was no obvious autophagy found here (Fig. 4A). However, more lipophagy in HSe0.3 group were observed using hepatopancreas ultrastructure (Fig. 4A).

To further confirm the activation of autophagy, the expression of autophagy genes and proteins in hepatopancreas was measured. As shown in Fig. 4, the expression of autophagy-related genes (*Beclin1*, *LC3*, *ATG7*, *ATG12* and *Rab7*) and the ratio of LC3-II to LC3-I were dramatically inhibited in HFD group compared to Con group, suggesting that HFD obviously inhibited the activity of autophagy ($P < 0.05$) (Fig. 4B to D). Dietary Se significantly upregulated the expression of autophagy-related genes (*Beclin1*, *LC3*, *ATG5*, *ATG7*, *ATG12* and *Rab7*) and the ratio of LC3-II to LC3-I ($P < 0.05$) (Fig. 4B to D).

3.2. In vitro study

3.2.1. Sodium selenite reduces oleic acid-induced lipid accumulation in grass carp hepatocyte

To investigate the mechanisms of Se affecting lipid metabolism, we performed a series of in vitro experiments using grass carp hepatocytes L8824. The results of the previous pre-experiments showed that less than 300 μM OA and no more than 100 μM sodium selenite did not adversely affect the viability of hepatocytes. Therefore, 300 μM OA and 100 μM sodium selenite were used in the vitro experiments.

The result of cell TG content shown that OA treatment significantly increased the TG content of L8824 ($P < 0.05$) (Fig. 5A), while sodium selenite obviously reduced cell TG content ($P < 0.05$) (Fig. 5A). Moreover, these were corroborated with hepatocytes Nile Red staining (Fig. 5B). More LD stained red by Nile Red were found in OA group, but sodium selenite can reduce the accumulation of LD (Fig. 5B). In addition, Western blotting results showed that OA treatment significantly inhibited ATG5 and LC3-II protein expression, but increased the expression of P62 protein in L8824 ($P < 0.05$)

(Fig. 5C and D). On the contrary, sodium selenite supplement effectively increased ATG5 and LC3-II protein expression and inhibited intracellular accumulation of protein P62 in L8824 ($P < 0.05$) (Fig. 5C and D).

3.2.2. Sodium selenite reduces lipid accumulation through lipophagy

To demonstrate whether lipophagy induced by Se is involved in reducing the OA-induced lipid accumulation in L8824, we used the autophagy inhibitor CQ to inhibit the autophagic pathway. The result showed that OA treatment significantly increased the TG content of hepatocytes ($P < 0.05$) (Fig. 6A) and the addition of sodium selenite significantly decreased hepatocytes TG content ($P < 0.05$) (Fig. 6A). However, with the addition of the autophagy inhibitor CQ, there was a significant increase in TG content of hepatocytes ($P < 0.05$) (Fig. 6A), which severely blocked the reduction effect of sodium selenite on lipid accumulation in L8824. Besides, LD in L8824 were visualized by Nile Red staining, which also suggested that the ability of sodium selenite to mitigate hepatic lipid accumulation was highly associated with autophagy (Fig. 6B). Furthermore, compared to the control, OA treatment inhibited the expression of autophagy-related genes (*Beclin1*, *ATG5*, *ATG7*, *ATG12*, *LC3*), while sodium selenite addition increased the expression of autophagy-related genes (*Beclin1*, *ATG5*, *ATG7*, *LC3* and *Rab7*) ($P < 0.05$) (Fig. 6C). And, the addition of autophagy inhibitor CQ significantly increased the expression of autophagy-related genes ($P < 0.05$) (Fig. 6C). The results of immunofluorescence co-localization indicated that OA inhibited the occurrence of autophagy, and there was no significant co-localization of LD with autophagosomes (Fig. 6D). Furthermore, the addition of CQ aggravated lipid accumulation and there was also no significant co-localization (Fig. 6D). Sodium selenite treatment increased the occurrence of autophagy and increased the co-localization of LD with autophagosomes (Fig. 6D). In addition, the addition of
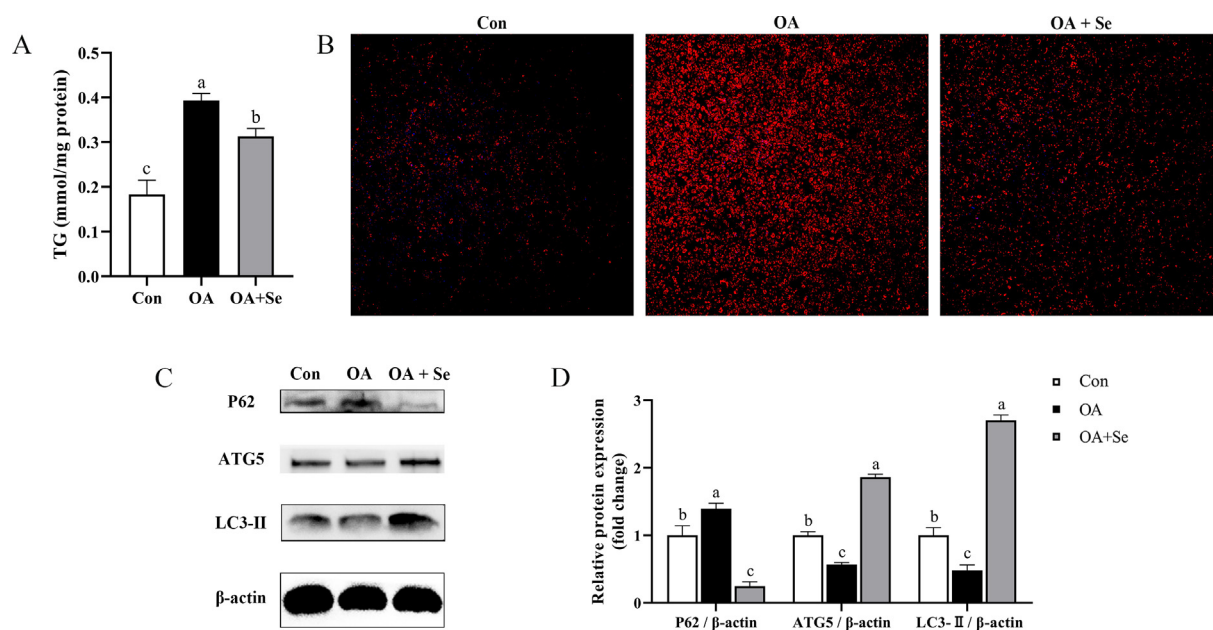

Fig. 5. Effects of sodium selenite on oleic acid (OA) induced lipid accomplishment in grass carp hepatocytes L8824. (A) Content variation of triglyceride (TG) in grass carp hepatocyte L8824. (B) Grass carp hepatocytes L8824 Nile Red staining. (C) Image of autophagy-related proteins in the grass carp hepatocyte L8824 evaluated by Western blotting analysis. (D) Relative quantification of autophagy-related proteins in the grass carp hepatocyte L8824. All results are shown as mean ± SD, $n = 3$. Different letters indicate significant differences based on one-way ANOVA by Duncan's test ($P < 0.05$). Con, no additional supplement; OA, 300 μM OA; OA + Se, 300 μM OA + 100 μM Na$_2$SeO$_3$. P62 = sequestosome 1; ATG5 = autophagy-related gene 5; LC3 = microtubule-associated protein light chain 3.
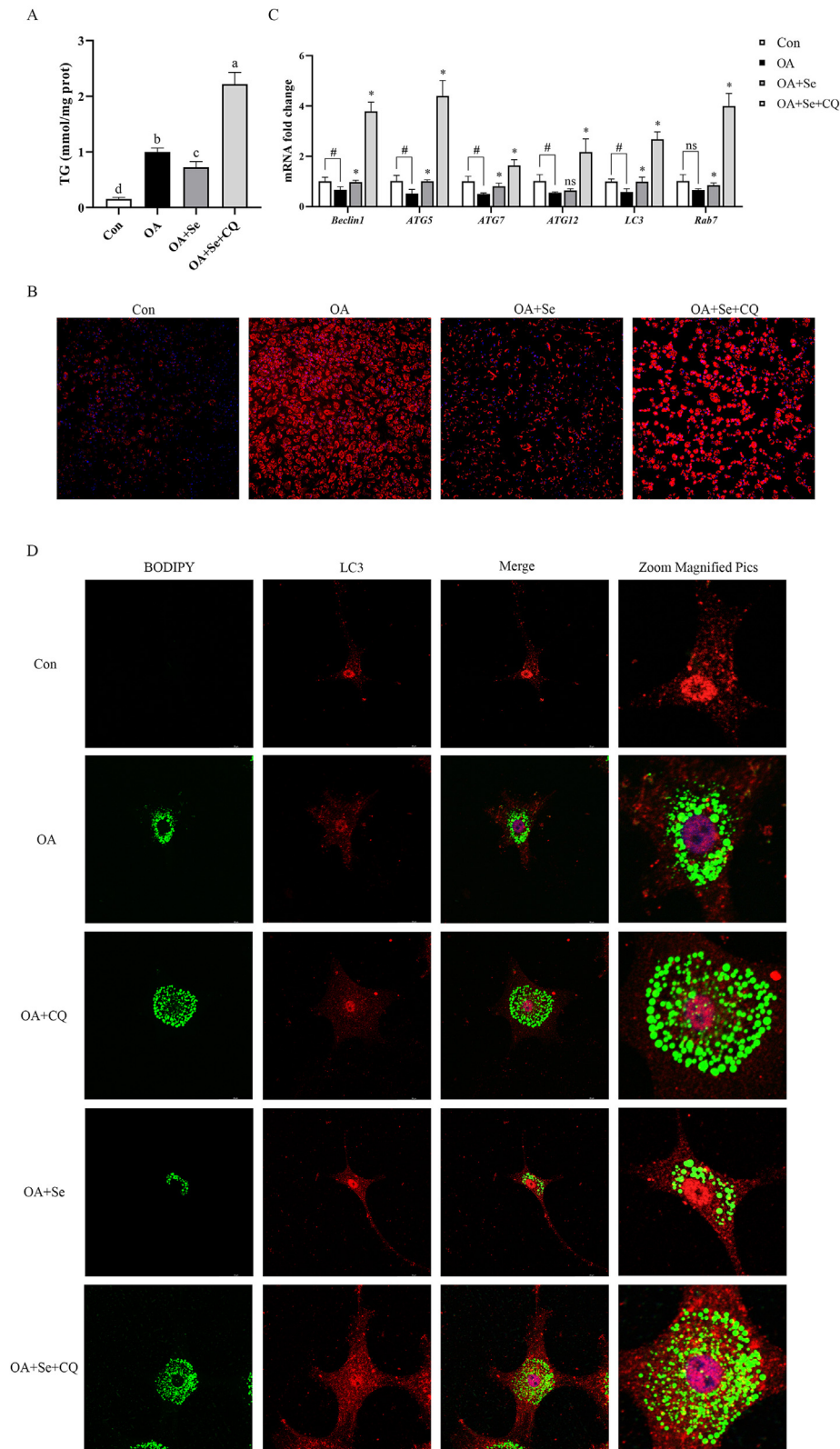
Fig. 6. Effects of lipophagy on the mitigation of lipid deposition by sodium selenite in L8824. (A) Content variation of triglyceride (TG) in grass carp hepatocyte L8824. (B) Grass carp hepatocytes L8824 Nile Red staining. (C) Expression of autophagy-related genes in grass carp hepatocyte L8824. (D) Co-localization of BODIPY 493/503 (green) with LC3 (red) in grass carp hepatocyte L8824. Nucleus are highlighted with 4,6-diamidino-2-phenylindole (DAPI). All results are shown as mean ± SD, $n = 3$. Different letters indicate significant differences based on one-way ANOVA by Duncan's test in (A) ($P < 0.05$). *$P < 0.05$ versus OA; #$P < 0.05$ versus Con by two-tailed t-test in (C). Con, no additional supplement; OA, 300 μM OA; OA + CQ, 300 μM OA + 50 μM CQ; OA + Se, 300 μM OA + 100 μM Na$_2$SeO$_3$; OA + Se + CQ, 300 μM OA + 100 μM Na$_2$SeO$_3$ + 50 μM CQ. OA = oleic acid; CQ = chloroquine; *Beclin1* = autophagy-related gene 6; *ATG5* = autophagy-related gene 5; *ATG7* = autophagy-related gene 7; *ATG12* = autophagy-related gene 12; *LC3* = microtubule-associated protein light chain 3; *Rab7* = ras-related protein 7.

autophagy inhibitor CQ further increased the co-localization of LD with autophagosomes (Fig. 6D), which indicated that sodium selenite increased autophagic flux.

4. Discussion

At present, research on Se mainly focuses on its excellent antioxidant ability, and only a few studies have shown its potential ability to regulate lipid metabolism in mice (Gao et al., 2020; Yi et al., 2020). In this study, we found that Se effectively relieved lipid accumulation induced by HFD by activating lipophagy.

It has also shown that long-term feeding of HFD inhibited the growth performance of fish (Cao et al., 2020; Li et al., 2016). In this study, we also found that long-term feeding of HFD decreased FBW, WGR and SGR, and it increased FCR, severely limiting the growth performance of grass carp, which also suggested that HFD inhibited the growth of grass carp. Previous studies also reported that Se could improve the growth performance of red sea bream (*Pagrus major*), tilapia (*O. niloticus*) and common carp (*Cyprinus carpio*) (Ashouri et al., 2015; Dawood et al., 2019; Iqbal et al., 2020). In the present study, the supplement of nano-Se significantly increased the WGR and reduced the FCR, suggesting that nano-Se enhanced the growth performance of grass carp fed HFD.

The use of HFD usually causes excessive lipid accumulation in fish and eventually induces fatty liver (Cao et al., 2020; He et al., 2015). In this study, higher serum TG as well as hepatopancreas TG was observed in HFD group, and we also found that HFD group has higher IPF and HSI. In addition, more LD were found in hepatopancreas of grass carp fed HFD. These results showed that HFD induced abnormal lipid accumulation in the hepatopancreas of grass carp. This is consistent with the study of Li et al. (2016) in grass carp. Similarly, HFD also induced excessive lipid accumulation in other fish, including blunt snout bream (*M. amblycephala*), largemouth bass (*Micropterus salmoides*) and common carp (*C. carpio*) (Abasubong et al., 2018; Dai et al., 2019; Xie et al., 2020).

Previous studies reported that the addition of Se relieved the adverse effects of HFD on mammals and prevented fatty liver disease (Kang et al., 1998; Sarkar et al., 2015). In this study, the supplement of nano-Se in HFD decreased serum TG and hepatopancreas TG content, and lower IPF and HSI were observed in HSe0.3 group. This is consistent with our previous research results (Liu et al., 2021). Besides, we found that nano-Se reduced the number of LD in the hepatopancreas of grass carp fed HFD. These results showed that nano-Se reduced HFD-induced hepatic lipid accumulation. Further, we verified the effect of Se on lipid metabolism in L8824. We found that OA treatment significantly increased cell TG content and the number of LD in L8824, causing abnormal lipid accumulation. The result indicated that the OA cell model was constructed successfully and a similar model was reported by a previous study (Lu et al., 2020). Following this, sodium selenite was added to treat OA-incubated hepatocytes. And the results showed that sodium selenite significantly decreased hepatocytes TG levels and reduced the number of LD, relieving the OA-induced lipid accumulation in L8824. Therefore, combining the results of in vivo and in vitro experiments, Se alleviated the excessive lipid accumulation induced by HFD.

Lipophagy is a selective autophagy that specifically breaks down LD in the cytoplasm. It plays an important role in lipid metabolism in animals. More and more studies have shown that lipophagy has great potential in improving hepatic steatosis and preventing fatty liver (Flores-Toro et al., 2016; Lu and Cederbaum, 2015; Singh et al., 2009). However, long-term high lipid stress greatly inhibits the occurrence of autophagy and blocks the participation of lipophagy in lipid metabolic processes, which in turn further exacerbates the abnormal deposition of lipids in the liver and eventually induces

fatty liver disease (Wu et al., 2019). In this study, lipophagy was observed in HSe0.3 group by a transmission electron microscope, which suggested that the reducing effect of nano-Se on lipid accumulation probably was associated with the activation of lipophagy. Thus, to clarify the role of lipophagy in reducing effect of Se on hepatic lipid accumulation, further studies were conducted. In this study, HFD decreased the expression of autophagy-related genes (*Beclin1*, *LC3*, *ATG7*, *ATG12* and *Rab7*) and reduced the ratio of protein LC3-II to protein LC3-I, which verified that autophagy was inhibited in HFD group. In a previous study, the expression of autophagy-related genes was also decreased in Tilapia (*O. niloticus*) fed HFD (Jia et al., 2020b). In addition, HFD also blocked autophagy in mice and excessive lipid accumulation was relieved with the activation of autophagy (Ding et al., 2017; Wang et al., 2017a). In the present study, nano-Se supplementation enhanced the expression of autophagy-related genes (*Beclin1*, *LC3*, *ATG5*, *ATG7*, *ATG12*, and *Rab7*) and increased the ratio of protein LC3-II to protein LC3-I, which suggested that nano-Se activated autophagy. In previous studies, Se maintained normal life activities of organisms by activating autophagy and selective autophagy in mammals (Li et al., 2015; Zhang et al., 2019), which is consistent with this study. Next, the effect of Se on autophagy in L8824 was examined in this study. In our vitro experiments, OA treatment was found to depress the expression of autophagy-related genes (*Beclin1*, *ATG5*, *ATG7*, *ATG12* and *LC3*). In addition, OA treatment increased the expression of protein P62 and decreased the expression of proteins ATG5 and LC3 in L8824. These results suggested that OA severely inhibited autophagy, which probably resulted in lipid accumulation. In previous studies, OA treatment depressed autophagy in HepG2 and AML12 cells, and cell TG content was also increased (Huang et al., 2017; Zhang et al., 2020). Interestingly, once the inhibition of autophagy was released, the abnormal lipid accumulation and lipotoxicity of HepG2 and AML12 cell were alleviated (Huang et al., 2017; Zhang et al., 2020). In this study, sodium selenite enhanced the expression of autophagy-related genes (*Beclin1*, *ATG5*, *ATG7*, *LC3* and *Rab7*). Sodium selenite reduced accumulation of protein P62 in cells and increased the expression of ATG5 and LC3-II. These results indicated that Se greatly restored autophagy inhibited by OA, and it was consistent with the results of in vivo experiments. The autophagy inhibitor CQ was a widely used inhibitor, which blocked autophagy and lipophagy via regulating lysosomal activity (Wang et al., 2019), so CQ was used to further clarify the importance of lipophagy. Firstly, sodium selenite restored the autophagy inhibited by OA in L8824 cells. Secondly, sodium selenite significantly reduced intracellular lipid accumulation in hepatocytes. Importantly, with the addition of the autophagy inhibitor CQ, this ameliorating effect of sodium selenite on lipid accumulation was diminished, which indicated that autophagy directly involved in the reducing effect of sodium selenite on lipid accumulation. Thirdly, sodium selenite increased co-localization between autophagosome and LD, whereas the OA treatment blocked the co-localization between autophagosome and LD. Especially, this improved effect of sodium selenite was again eliminated by the autophagy inhibitor CQ, suggesting that lipophagy, a selective autophagy, played a particularly important role in the beneficial effect of sodium selenite on lipid accumulation. The cell experiments in this study provided important evidence that Se enhanced lipophagy activity, and lipophagy was directly involved in reducing TG levels in hepatocytes.

5. Conclusion

In conclusion, this study suggests that Se significantly mitigates excessive lipid accumulation in grass carp fed HFD, and to the best of our knowledge, this is the first study that proves that the

potential molecular mechanism of the effect of Se on reducing hepatopancreas lipid accumulation is associated with the activation of lipophagy, thus this study provides a new solution to mitigate the adverse effects of HFD on fish.

Author contributions

Xiaotian Zhang: Methodology, Investigation, Data curation, Writing original draft, Formal analysis. **Haibo Yu:** Conceptualization, Methodology, Resources, Supervision, Project administration, Funding acquisition, Writing – review & editing. **Xianfang Yan:** Methodology, Investigation, Data curation. **Pengju Li:** Methodology, Investigation, Data curation. **Chi Wang:** Investigation. **Cheng Zhang:** Investigation. **Hong Ji:** Resources.

Declaration of competing interest

We declare that we have no financial and personal relationships with other people or organizations that can inappropriately influence our work, and there is no professional or other personal interest of any nature or kind in any product, service and/or company that could be construed as influencing the content of this paper.

Acknowledgment

References

Abasubong KP, Li XF, Zhang DD, Jia ET, Xiang-Yang Y, Xu C, Liu WB. Dietary supplementation of xylooligosaccharides benefits the growth performance and lipid metabolism of common carp (*Cyprinus carpio*) fed high-fat diets. Aquacult Nutr 2018;24(5):1416–24. https://doi.org/10.1111/anu.12678.

Ashouri S, Keyvanshokooh S, Salati AP, Johari SA, Pasha-Zanoosi H. Effects of different levels of dietary selenium nanoparticles on growth performance, muscle composition, blood biochemical profiles and antioxidant status of common carp (*Cyprinus carpio*). Aquaculture 2015;446:25–9. https://doi.org/10.1016/j.aquaculture.2015.04.021.

Avery JC, Hoffmann PR. Selenium, selenoproteins, and immunity. Nutrients 2018;10(9):1203. https://doi.org/10.3390/nu10091203.

Cao XF, Liu WB, Ai QH, Li XS, Li JB, Fang W, Huang YY, Wang CC, Jiang GZ. High-fat diet-induced inflammation aggravates hepatic steatosis of blunt snout bream (*Megalobrama amblycephala*) through the transcription regulation of fatty acid synthesis and oxidation. Aquacult Nutr 2020;26(5):1493–504. https://doi.org/10.1111/anu.13097.

Chen QQ, Liu WB, Zhou M, Dai YJ, Xu C, Tian HY, Xu WN. Effects of berberine on the growth and immune performance in response to ammonia stress and high-fat dietary in blunt snout bream *Megalobrama amblycephala*. Fish Shellfish Immunol 2016;55:165–72. https://doi.org/10.1016/j.fsi.2016.05.023.

Cisa-Wieczorek S, Hernandez-Alvarez MI. Deregulation of lipid homeostasis: a fa(c)t in the development of metabolic diseases. Cells 2020;9(12):2605. https://doi.org/10.3390/cells9122605.

Dai YJ, Cao XF, Zhang DD, Li XF, Liu WB, Jiang GZ. Chronic inflammation is a key to inducing liver injury in blunt snout bream (*Megalobrama amblycephala*) fed with high-fat diet. Dev Comp Immunol 2019;97:28–37. https://doi.org/10.1016/j.dci.2019.03.009.

Dawood MAO, Koshio S, Zaineldin AI, Van Doan H, Ahmed HA, Elsabagh M, Abdel-Daim MM. An evaluation of dietary selenium nanoparticles for red sea bream (*Pagrus major*) aquaculture: growth, tissue bioaccumulation, and antioxidative responses. Environ Sci Pollut Res 2019;26(30):30876–84. https://doi.org/10.1007/s11356-019-06223-6.

Deng KY, Pan MZ, Liu JH, Yang MX, Gu ZX, Zhang Y, Liu GX, Liu D, Zhang WB, Mai KS. Chronic stress of high dietary carbohydrate level causes inflammation and influences glucose transport through *SOCS3* in Japanese flounder *Paralichthys olivaceus*. Sci Rep 2018;8(1):1–13. https://doi.org/10.1038/s41598-018-25412-w.

Ding SB, Jiang JJ, Zhang GF, Bu YJ, Zhang GH, Zhao XM. Resveratrol and caloric restriction prevent hepatic steatosis by regulating SIRT1-autophagy pathway and alleviating endoplasmic reticulum stress in high-fat diet-fed rats. PLoS One 2017;12(8):e0183541. https://doi.org/10.1371/journal.pone.0183541.

Durigon EG, Kunz DF, Peixoto NC, Uczay J, Lazzari R. Diet selenium improves the antioxidant defense system of juveniles Nile tilapia (*Oreochromis niloticus* L.). Braz J Biol 2019;79(3):527–32. https://doi.org/10.1590/1519-6984.187760.

Flores-Toro JA, Go KL, Leeuwenburgh C, Kim JS. Autophagy in the liver: cell's cannibalism and beyond. Arch Pharm Res 2016;39(8):1050–61. https://doi.org/10.1007/s12272-016-0807-8.

Gao Y, Xu YQ, Ruan JY, Yin JF. Selenium affects the activity of black tea in preventing metabolic syndrome in high-fat diet-fed Sprague-Dawley rats. J Sci Food Agric 2020;100(1):225–34. https://doi.org/10.1002/jsfa.10027.

Ghazi S, Diab AM, Khalafalla MM, Mohamed RA. Synergistic effects of selenium and zinc oxide nanoparticles on growth performance, hemato-biochemical profile, immune and oxidative stress responses, and intestinal morphometry of Nile tilapia (*Oreochromis niloticus*). Biol Trace Elem Res 2022;200(1):364–74. https://doi.org/10.1007/s12011-021-02631-3.

Guo DY, Xie MQ, Xiao H, Xu LL, Zhang SY, Chen XX, Wu ZX. *Bacillus subtilis* supplementation in a high-fat diet modulates the gut microbiota and ameliorates hepatic lipid accumulation in grass carp (*Ctenopharyngodon idella*). Fishes 2022;7(3):94. https://doi.org/10.3390/fishes7030094.

Guo XZ, Liang XF, Fang L, Yuan XC, Zhou Y, Zhang J, Li B. Effects of dietary non-protein energy source levels on growth performance, body composition and lipid metabolism in herbivorous grass carp (*Ctenopharyngodon idella* Val.). Aquacult Res 2015;46(5):1197–208. https://doi.org/10.1111/are.12275.

Hao JY, Lin Y, Pan WJ, Jiang WQ, Liu B, Miao LH, Zhou QL, Liang HL, Ge XP. Dietary selenium enhances the growth and anti-oxidant capacity of juvenile blunt snout bream (*Megalobrama amblycephala*). Fish Shellfish Immunol 2020;101: 115–25. https://doi.org/10.1016/j.fsi.2020.03.041.

He AY, Ning LJ, Chen LQ, Chen YL, Xing Q, Li JM, Qiao F, Li DL, Zhang ML, Du ZY. Systemic adaptation of lipid metabolism in response to low- and high-fat diet in Nile tilapia (*Oreochromis niloticus*). Physiol Rep 2015;3(8):e12485. https://doi.org/10.14814/phy2.12485.

Huang Q, Wang T, Yang L, Wang HY. Ginsenoside Rb2 alleviates hepatic lipid accumulation by restoring autophagy via induction of Sirt1 and activation of AMPK. Int J Mol Sci 2017;18(5):1063. https://doi.org/10.3390/ijms18051063.

Ibrahim MS, El-gendy GM, Ahmed AI, Elharoun ER, Hassaan MS. Nanoselenium versus bulk selenium as a dietary supplement: effects on growth, feed efficiency, intestinal histology, haemato-biochemical and oxidative stress biomarkers in Nile tilapia (*Oreochromis niloticus Linnaeus*, 1758) fingerlings. Aquacult Res 2021;52(11):5642–55. https://doi.org/10.1111/are.15439.

Iqbal S, Atique U, Mahboob S, Haider MS, Iqbal HS, Al-Ghanim KA, Al-Misned F, Ahmed Z, Mughal MS. Effect of supplemental selenium in fish feed boosts growth and gut enzyme activity in juvenile tilapia (*Oreochromis niloticus*). J King Saud Univ Sci 2020;32(5):2610–6. https://doi.org/10.1016/j.jksus.2020.05.001.

Jia R, Cao LP, Du JL, He Q, Gu ZY, Jeney G, Xu P, Yin GJ. Effects of high-fat diet on antioxidative status, apoptosis and inflammation in liver of tilapia (*Oreochromis niloticus*) via Nrf2, TLRs and JNK pathways. Fish Shellfish Immunol 2020a;104: 391–401. https://doi.org/10.1016/j.fsi.2020.06.025.

Jia R, Cao LP, Du JL, He Q, Gu ZY, Jeney G, Xu P, Yin GJ. Effects of high-fat diet on steatosis, endoplasmic reticulum stress and autophagy in liver of tilapia (*Oreochromis niloticus*). Front Mar Sci 2020b;7:363. https://doi.org/10.3389/fmars.2020.00363.

Kang BPS, Bansal MP, Mehta U. Selenium supplementation and diet induced hypercholesterolemia in the rat: changes in lipid levels, malonyldialdehyde production and the nitric oxide synthase activity. Gen Physiol Biophys 1998;17(1):71–8.

Khurana A, Tekula S, Saifi MA, Venkatesh P, Godugu C. Therapeutic applications of selenium nanoparticles. Biomed Pharmacother 2019;111:802–12. https://doi.org/10.1016/j.biopha.2018.12.146.

Kumar N, Krishnani KK, Singh NP. Oxidative and cellular stress as bioindicators for metal contamination in freshwater mollusk *Lamellidens marginalis*. Environ Sci Pollut Res 2017;24(19):16137–47. https://doi.org/10.1007/s11356-017-9266-0.

Kumar N, Singh NP. Effect of dietary selenium on immuno-biochemical plasticity and resistance against *Aeromonas veronii biovar sobria* in fish reared under multiple stressors. Fish Shellfish Immunol 2019;84:38–47. https://doi.org/10.1016/j.fsi.2018.09.065.

Kursvietiene L, Mongirdiene A, Bernatoniene J, Sulinskiene J, Staneviciene I. Selenium anticancer properties and impact on cellular redox status. Antioxidants 2020;9(1):80. https://doi.org/10.3390/antiox9010080.

Li AX, Yuan XC, Liang XF, Liu LW, Li J, Li B, Fang JG, Li J, He S, Xue M, Wang J, Tao YX. Adaptations of lipid metabolism and food intake in response to low and high fat diets in juvenile grass carp (*Ctenopharyngodon idellus*). Aquaculture 2016;457: 43–9. https://doi.org/10.1016/j.aquaculture.2016.01.014.

Li J, Qi W, Chen G, Feng D, Liu JH, Ma B, Zhou CQ, Mu CL, Zhang WL, Chen Q, Zhu YS. Mitochondrial outer-membrane E3 ligase MUL1 ubiquitinates ULK1 and regulates selenite-induced mitophagy. Autophagy 2015;11(8):1216–29. https://doi.org/10.1080/15548627.2015.1017180.

Li XF, Jiang YY, Liu WB, Ge XP. Protein-sparing effect of dietary lipid in practical diets for blunt snout bream (*Megalobrama amblycephala*) fingerlings: effects on digestive and metabolic responses. Fish Physiol Biochem 2012;38(2):529–41. https://doi.org/10.1007/s10695-011-9533-9.

Liu GH, Yu HB, Wang C, Li PJ, Liu S, Zhang XT, Zhang C, Qi M, Ji H. Nano-selenium supplements in high-fat diets relieve hepatopancreas injury and improve survival of grass carp *Ctenopharyngodon idella* by reducing lipid deposition. Aquaculture 2021;538:736580. https://doi.org/10.1016/j.aquaculture.2021.736580.

Liu S, Yu HB, Li PJ, Wang C, Liu GH, Zhang XT, Zhang C, Qi M, Ji H. Dietary nano-selenium alleviated intestinal damage of juvenile grass carp (*Ctenopharyngodon idella*) induced by high-fat diet: insight from intestinal morphology, tight junction, inflammation, anti-oxidization and intestinal microbiota. Anim Nutr 2022;8(1):235–48. https://doi.org/10.1016/j.aninu.2021.07.001.

Lu JM, Li SD, He XG, Tang R, Li DP. An in-pond tank culture system for high-intensive fish production: effect of stocking density on growth of grass carp (*Cteno-pharyngodon idella* Valenciennes, 1844) and blunt snout bream (*Megalobrama amblycephala* Yih, 1955). Aquaculture 2022;549:737808. https://doi.org/10.1016/j.aquaculture.2021.737808.

Lu KL, Xu WN, Li JY, Li XF, Huang GQ, Liu WB. Alterations of liver histology and blood biochemistry in blunt snout bream *Megalobrama amblycephala* fed high-fat diets. Fish Sci 2013a;79(4):661–71. https://doi.org/10.1007/s12562-013-0635-4.

Lu KL, Xu WN, Li XF, Liu WB, Wang LN, Zhang CN. Hepatic triacylglycerol secretion, lipid transport and tissue lipid uptake in blunt snout bream (*Megalobrama amblycephala*) fed high-fat diet. Aquaculture 2013b;408:160–8. https://doi.org/10.1016/j.aquaculture.2013.06.003.

Lu RH, Qin CB, Yang F, Zhang WY, Zhang YR, Yang GK, Yang LP, Meng XL, Yan X, Nie GX. Grape seed proanthocyanidin extract ameliorates hepatic lipid accumulation and inflammation snout in grass carp (*Ctenopharyngodon idella*). Fish Physiol Biochem 2020;46(5):1665–77. https://doi.org/10.1007/s10695-020-00819-3.

Lu YK, Cederbaum AI. Autophagy protects against CYP2E1/chronic ethanol-induced hepatotoxicity. Biomolecules 2015;5(4):2659–74. https://doi.org/10.3390/biom5042659.

Ma Q, Li LY, Le JY, Lu DL, Qiao F, Zhang ML, Du ZY, Li DL. Dietary microencapsulated oil improves immune function and intestinal health in Nile tilapia fed with high-fat diet. Aquaculture 2018;496:19–29. https://doi.org/10.1016/j.aquaculture.2018.06.080.

Sarkar B, Bhattacharjee S, Daware A, Tribedi P, Krishnani KK, Minhas PS. Selenium nanoparticles for stress-resilient fish and livestock. Nanoscale Res Lett 2015;10:1–14. https://doi.org/10.1186/s11671-015-1073-2.

Singh R, Kaushik S, Wang YJ, Xiang YQ, Novak I, Komatsu M, Tanaka K, Cuervo AM, Czaja MJ. Autophagy regulates lipid metabolism. Nature 2009;458(7242):1131–5. https://doi.org/10.1038/nature07976.

Tian JJ, Jin YQ, Yu EM, Sun JH, Xia Y, Zhang K, Li ZF, Gong WB, Wang GJ, Xie J. Farnesoid X receptor is an effective target for modulating lipid accumulation in grass carp, *Ctenopharyngodon idella*. Aquaculture 2021;534:736248. https://doi.org/10.1016/j.aquaculture.2020.736248.

Ueno T, Komatsu M. Autophagy in the liver: functions in health and disease. Nat Rev Gastroenterol Hepatol 2017;14(3):170–84. https://doi.org/10.1038/nrgastro.2016.185.

Wang H, Zhu YY, Wang L, Teng T, Zhou M, Wang SG, Tian YZ, Du L, Yin XX, Sun Y. Mangiferin ameliorates fatty liver via modulation of autophagy and inflammation in high-fat-diet induced mice. Biomed Pharmacother 2017a;96:328–35. https://doi.org/10.1016/j.biopha.2017.10.022.

Wang J, Han SL, Li LY, Lu DL, Limbu SM, Li DL, Zhang ML, Du ZY. Lipophagy is essential for lipid metabolism in fish. Sci Bull 2018;63(14):879–82. https://doi.org/10.1016/j.scib.2018.05.026.

Wang J, Han SL, Lu DL, Li LY, Limbu SM, Li DL, Zhang ML, Du ZY. Inhibited lipophagy suppresses lipid metabolism in zebrafish liver cells. Front Physiol 2019;10:1077. https://doi.org/10.3389/fphys.2019.01077.

Wang N, Tan HY, Li S, Xu Y, Guo W, Feng YB. Supplementation of micronutrient selenium in metabolic diseases: its role as an antioxidant. Oxid Med Cell Longev 2017b;2017. https://doi.org/10.1155/2017/7478523.

Wei XL, Hogstrand C, Chen GH, Lv WH, Song YF, Xu YC, Luo Z. Zn induces lipophagy via the deacetylation of Beclin1 and alleviates Cu-induced lipotoxicity at their environmentally relevant concentrations. Environ Sci Technol 2021;55(8):4943–53. https://doi.org/10.1021/acs.est.0c08609.

Wu LX, Wei CC, Yang SB, Zhao T, Luo Z. Effects of fat and fatty acids on the formation of autolysosomes in the livers from yellow catfish *Pelteobagrus fulvidraco*. Genes 2019;10(10):751. https://doi.org/10.3390/genes10100751.

Wu SG, Wang GT, Angert ER, Wang WW, Li WX, Zou H. Composition, diversity, and origin of the bacterial community in grass carp intestine. PLoS One 2012;7(2):e30440. https://doi.org/10.1371/journal.pone.0030440.

Xia XJ, Wang X, Qin WH, Jiang JQ, Cheng LK. Emerging regulatory mechanisms and functions of autophagy in fish. Aquaculture 2019;511:734212. https://doi.org/10.1016/j.aquaculture.2019.734212.

Xiao PZ, Ji H, Ye YT, Zhang BT, Chen YS, Tian JJ, Liu P, Chen LQ, Du ZY. Dietary silymarin supplementation promotes growth performance and improves lipid metabolism and health status in grass carp (*Ctenopharyngodon idellus*) fed diets with elevated lipid levels. Fish Physiol Biochem 2017;43(1):245–63. https://doi.org/10.1007/s10695-016-0283-6.

Xie SW, Yin P, Tian LX, Yu YY, Liu YJ, Niu J. Dietary supplementation of astaxanthin improved the growth performance, antioxidant ability and immune response of juvenile largemouth bass (*Micropterus salmoides*) fed high-fat diet. Mar Drugs 2020;18(12):642. https://doi.org/10.3390/md18120642.

Yi HW, Zhu XX, Huang XL, Lai YZ, Tang Y. Selenium-enriched Bifidobacterium longum protected alcohol and high fat diet induced hepatic injury in mice. Chin J Nat Med 2020;18(3):169–77. https://doi.org/10.1016/S1875-5364(20)30018-2.

Zhang L, Yao ZM, Ji G. Herbal extracts and natural products in alleviating non-alcoholic fatty liver disease via activating autophagy. Front Pharmacol 2018;9:1459. https://doi.org/10.3389/fphar.2018.01459.

Zhang SQ, Xu JL, He ZS, Xue F, Jiang TB, Xu MZ. Sodium selenate ameliorates cardiac injury developed from high-fat diet in mice through regulation of autophagy activity. Sci Rep 2019;9(1):18752. https://doi.org/10.1038/s41598-019-54985-3.

Zhang T, Liu JX, Shen SN, Tong Q, Ma XJ, Lin LG. SIRT3 promotes lipophagy and chaperon-mediated autophagy to protect hepatocytes against lipotoxicity. Cell Death Differ 2020;27(1):329–44. https://doi.org/10.1038/s41418-019-0356-z.

Zhang XT, Yu HB, Yan XF, Li PJ, Wang C, Zhang C, Ji H, Gao QF, Dong SL. Selenium improved mitochondrial quality and energy supply in the liver of high-fat diet-fed grass carp (*Ctenopharyngodon idella*) after heat stress. Fish Physiol Biochem 2022;48(6):1701–16. https://doi.org/10.1007/s10695-022-01140-x.

Zhao H, Luo YE, Wu ZX, Zhou Y, Guo DY, Wang H, Chen XX. Hepatic lipid metabolism and oxidative stress responses of grass carp (*Ctenopharyngodon idella*) fed diets of two different lipid levels against *Aeromonas hydrophila* infection. Aquaculture 2019;509:149–58. https://doi.org/10.1016/j.aquaculture.2019.05.029.

Zhao T, Wu K, Hogstrand C, Xu YH, Chen GH, Wei CC, Luo Z. Lipophagy mediated carbohydrate-induced changes of lipid metabolism via oxidative stress, endoplasmic reticulum (ER) stress and ChREBP/PPAR gamma pathways. Cell Mol Life Sci 2020;77(10):1987–2003. https://doi.org/10.1007/s00018-019-03263-6.